Neutron-powder-diffraction study of the nuclear and magnetic structures of the antiferromagnetic superconductor $HoNi_2B_2C$

Q. Huang
Reactor Radiation Division, National Institute of Standards and Technology, Gaithersburg, Maryland 20899 and University of Maryland, College Park, Maryland 20742

A. Santoro
Reactor Radiation Division, National Institute of Standards and Technology, Gaithersburg, Maryland 20899

T. E. Grigereit and J. W. Lynn
Reactor Radiation Division, National Institute of Standards and Technology, Gaithersburg, Maryland 20899 and Center for Superconductivity Research, University of Maryland, College Park, Maryland 20742

R. J. Cava, J. J. Krajewski, and W. F. Peck, Jr.
AT&T Bell Laboratories, Murray Hill, New Jersey 07974
(Received 13 June 1994)

The nuclear and magnetic structures of $HoNi_2B_2C$ have been investigated by neutron-powder-diffraction methods at room temperature and at 10, 5.1, and 2.2 K. The compound crystallizes with the symmetry of space group $I4/mmm$ and lattice parameters $a=3.5170(1)$ and $c=10.5217(3)$ Å, at room temperature. The structure may be regarded as formed of (HoC) layers with the rock salt configuration alternating with $(B)(Ni_2)(B)$ blocks having a fluorite-type arrangement of the atoms. No phase transition of the nuclear structure has been observed down to a temperature of 2.2 K. Magnetic peaks begin to appear at about 8 K. The magnetic structure is the superposition of two configurations, one in which ferromagnetic sheets of holmium spins parallel to the a,b plane are coupled antiferromagnetically along the c axis (magnetic space group $Pm'mm'$), and another in which ferromagnetic planes are rotated away from the antiparallel configuration to give an incommensurate helicoidal structure with a period approximately equal to 12 times the length of the c axis.

INTRODUCTION

The discovery of superconductivity in quaternary intermetallic compounds has been recently reported in a number of publications. A superconducting transition with onset temperature of 12.5 K has been found by Nagarajan *et al.*[1] in the system Y-Ni-B-C, and it has been suggested by Cava *et al.*[2] that the phase involved in the transition has the formula YNi_2B_2C. Superconductivity at 23 K has been discovered in the system Y-Pd-B-C by Cava *et al.*,[3] but the chemical composition of the superconducting material has not yet been determined with certainty. Single-phase quaternary compounds of formula LNi_2B_2C (with L=Lu, Tm, Er, Ho, Y, Dy, Tb, Sm, Ce, and La) have been prepared by Cava *et al.*[2] and found to have transition temperatures of 7.5, 10.5, and 11 K for the Ho, Er, and Tm compounds, respectively, and up to 16.6 K for $LuNi_2B_2C$, with a variation of only 1 K in going from Lu to Y. The crystal structure of $LuNi_2B_2C$ has been determined by Siegrist *et al.*[4] by single-crystal x-ray-diffraction analysis and it has been found to be a variant of the tetragonal body-centered $ThCr_2Si_2$-type structure with the Ni-B framework modified by the insertion of a carbon atom in the lanthanide layer.

A remarkable property of the LNi_2B_2C compounds is that superconductivity is observed not only in the materials which contain nonmagnetic elements, but also in those with heavy rare-earth magnetic atoms such as Tm, Er, and Ho. This behavior is similar, in some respects, to that observed in the RRh_4B_4 (Ref. 5) and RMo_6S_8 (Ref. 6) classes of materials (R=rare earth), where the crystallographic sites occupied by the magnetic ions are thought to be well isolated from the conduction paths so that the spin interaction between the local magnetic moments and the conduction electrons is too weak to inhibit superconductivity. In a study of the magnetic properties of LNi_2B_2C, with L=Tm, Er, and Ho, Eisaki *et al.*[7] have shown that antiferromagnetism and superconductivity do coexist in these boride-carbide compounds and that their competition produces a wide variety of interesting phenomena. Experiments with an applied magnetic field showed strong anomalies near the antiferromagnetic ordering temperature, including reentrant resistivity in some cases. The most pronounced anomalies were observed for $HoNi_2B_2C$ which, under fields below 0.2 T, has a transition to a superconducting state at temperatures well above 5 K. At about 5 K, a sharp resistivity peak appears, indicating a transition back to the normal nonsuperconducting state, associated with antiferromagnetic ordering of the Ho spins. Finally, at temperatures below 5 K, the compound regains its superconducting behavior.

0163-1829/95/51(6)/3701(8)/$06.00

TABLE I. Collection of intensity data.

Monochromatic beam:	311 reflection of Cu monochromator.
Wavelength:	1.539(1) Å
Horizontal divergences:	15′,20′,7′ of arc for the in-pile, monochromatic beam, and diffracted beam collimators, respectively.
Sample container:	V cans with 12 mm diameter for the 296, 10, and 2.2 K experiments, respectively. V annular can of 12 and 6 mm diameter for the 5.1-K experiment.
2θ angular range:	4°–164°, steps: 0.05°.
Scattering amplitudes (10^{-12} cm): (Refs. 10 and 11)	b(Ho)=0.808, b(Ni)=1.03, b(^{11}B)=0.665, b(C)=0.665, b(O)=0.581.
Measurements made at 296, 10, 5.1, and 2.2 K.	
Measured value of μr:	1.33 (at 296 K); 1.45 (at 10 and 2.2 K); 1.15 (at 5.1 K)

What is particularly significant in this compound, compared to other antiferromagnetic superconductors, is that the reentrant resistivity peak at 5 K is observed even in the absence of a magnetic field. The only antiferromagnet to exhibit reentrant behavior is $Tm_2Fe_3Si_5$,[8] but in that case superconductivity is not recovered at low temperature.

In order to understand the anomalous transitions described previously, and to relate them to the competition between magnetism and superconductivity, it is essential to have a precise knowledge of the nuclear and magnetic structures of the compounds involved. For this reason, we have carried out complete, high-resolution structural analyses of $HoNi_2B_2C$ at room temperature and near the transition points of 10, 5, and 2 K, using neutron-scattering techniques. Preliminary results of this analysis have shown[9] that two states of the magnetic structure are present in this system, an incommensurate helicoidally modulated one with a wave vector about 12 times the length of the c axis, and another one which is a commensurate antiferromagnet. Field- and temperature-dependent studies show that initially the amplitudes of both states are weak and grow together as the temperature decreases. Superconductivity appears at about 7.5 K and, upon further cooling, at the reentrant transition ($\sim$5 K) the modulated component decreases sharply in favor of the commensurate antiferromagnetic component. Superconductivity then reappears and coexists with antiferromagnetism to low temperatures. From these observations it was concluded that the modulated state is detrimental to superconductivity in this system, since the misalignment of the spins in adjacent ferromagnetic planes destroys the antiferromagnetic compensation of the Ni layers, located between holmium, and produces a net ferromagnetic component on these superconducting Ni layers. In the following sections of this paper, we report a detailed analysis of the nuclear and magnetic structures of $HoNi_2B_2C$ at appropriately selected temperatures.

EXPERIMENTAL

The sample used in this study was prepared by arc-melting and subsequent annealing, as described in Ref. 2,

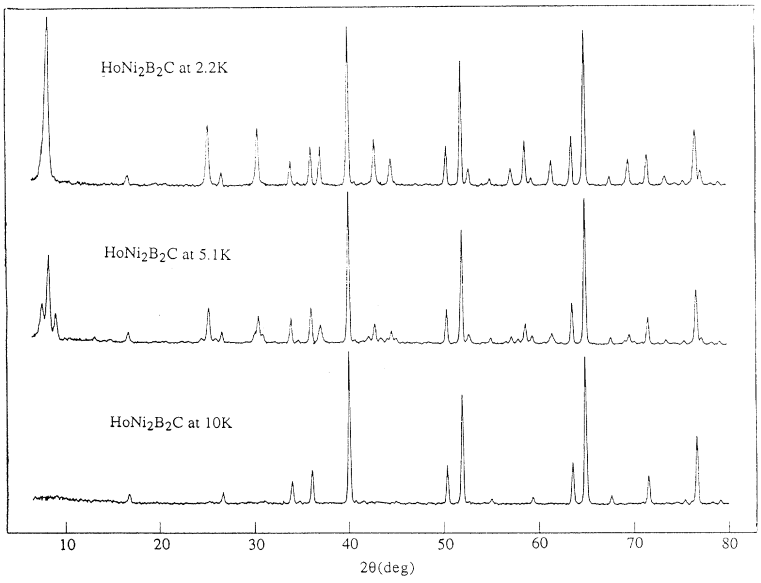

FIG. 1. Powder patterns of $HoNi_2B_2C$ at 2.2, 5.1, and 10 K. The satellites of the modulated magnetic structure are well separated from the central peaks due to the antiferromagnetic ordering in the pattern at 5.1 K. In the pattern at 2.2 K, however, they are closer to the central peaks and weaker than at 5.1 K, while the antiferromagnetic peaks have grown dramatically in intensity.

using boron in the starting materials that was enriched to 98.5% with the isotope ^{11}B to reduce nuclear absorption.

The neutron-powder-diffraction measurements were made using the new high-resolution 32-counter diffractometer of the National Institute of Standards and Technology, with the experimental conditions listed in Table I. Plots of a portion of the raw data taken at 10, 5.1, and 2.2 K are compared in Fig. 1 to show the evolution of the magnetic peaks in the powder patterns. The diffraction lines observed at room temperature and 10 K were readily indexed on a tetragonal cell with lattice parameters close to those determined for $LuNi_2B_2C$.[4] A few very weak extra lines showed that impurity phases in the sample are less than about 2% and demonstrate the high quality of the sample (one of the impurity phases was magnetically ordered with a magnetic Bragg peak at about $2\theta=5.5$ and a transition temperature a few degrees above 10 K). The observed intensities were corrected for absorption using the measured transmission factors listed in Table I for the various experiments. All refinements of the nuclear and magnetic structures were carried out with the GSAS program of Larson and Von Dreele.[11]

A. Refinement of the nuclear structure at room temperature and at 10 K

The nuclear structure of $HoNi_2B_2C$ was refined above the magnetic ordering temperature assuming the symme-

TABLE II. Structural parameters for $HoNi_2B_2C$ at 296, 10, 5.1, and 2.2 K. (Top) Nuclear structure: Space group: $I4/mmm$; Atomic positions: Ho(0,0,0), Ni(1/2,0,1/4), B(0,0,z), and C(1/2,1/2,0). All magnetic peaks were excluded in the refinenments using the data collected at 5.1 and 2.2 K. (Middle) Magnetic structure at 5.1 K ($5° \le 2\theta \le 100°$) and 2.2 K ($5° \le 2\theta \le 80°$). The nuclear structure was included in the refinements. $M1$ indicates the antiferromagnetic structure with symmetry of $Pm'mm'$ and $a_{M1}=b_{M1}=a_N$, $c_{M1}=c_N$ and $M2$ the spiral structure with $a_{M2}=b_{M2}=a_N$, $c_{M2}=nc_N$, and $\phi=360°/n$. (Bottom) Selected interatomic distances (< 3.0) (Å).

	296 K	10 K	5.1 K	2.2 K
a_N (Å)	3.5170(1)	3.50866(4)	3.5087(1)	3.50834(4)
c_N (Å)	10.5217(3)	10.5274(2)	10.5272(5)	10.5272(3)
V (Å^3)	130.15(1)	129.588(4)	129.60(2)	129.573(4)
Ho B (Å^2)	0.18(3)	0.10(3)	0.06(3)	0.14(2)
Ni B (Å^2)	0.53(2)	0.36(2)	0.32(3)	0.40(2)
B z	0.3589(1)	0.3592(2)	0.3586(2)	0.3588(2)
B (Å^2)	0.77(3)	0.57(3)	0.65(4)	0.61(4)
C B (Å^2)	0.73(4)	0.67(4)	0.72(4)	0.68(4)
R_p (%)	5.19	5.41	5.16	5.77
R_{wp} (%)	6.59	7.28	7.08	7.90
χ	1.39	1.39	1.73	1.52

	5.1 K		2.2 K	
	$M1$	$M2$	$M1$	$M2$
ϕ(°)		30		25.71
n		12		14
μ_x	0	$7.1\sin[m^a(180-\phi/2)]\mu_B$	0	$8.7\sin[m(180-\phi/2)]\mu_B$
μ_y	$\pm 7.1(1)\mu_B$	$7.1\cos[m(180-\phi/2)]\mu_B$	$\pm 8.7(1)\mu_B$	$8.7\cos[m(180-\phi/2)]\mu_B$
μ_z	0	0	0	0
μ	$7.1(1)\mu_B$	$7.1(1)\mu_B$	$8.7(1)\mu_B$	$8.7(1)\mu_B$
Phase fraction (wt. %):	51(1)	49(1)	85(1)	15(1)
R_p (%)		8.03		10.44
R_{wp} (%)		9.50		11.85
χ		1.94		1.74

	296 K	10 K	5.1 K	2.2 K
Ho-B	2.8964(8)	2.8902(9)	2.893(1)	2.892(1)
Ho-C	2.48690(8)	2.48100(3)	2.4810(1)	2.48077(3)
Ni-Ni	2.48690(8)	2.48100(3)	2.4810(1)	2.48077(3)
Ni-B	2.0988(9)	2.0971(9)	2.094(1)	2.095(1)
B-C	1.485(2)	1.483(2)	1.489(2)	1.486(2)

[a] $m=0,1,\ldots,2n-1$.

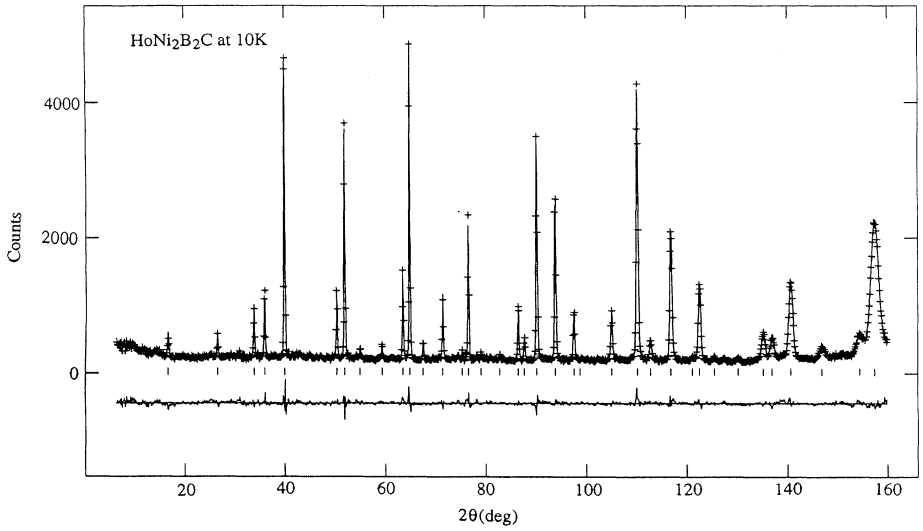

FIG. 2. Observed and calculated pattern after refinement of the nuclear structure of $HoNi_2B_2C$ at 10 K. The difference plot is represented in the lower part of the figure.

try of space group $I4/mmm$ and using as initial parameters those found by Siegrist *et al.* for $LuNi_2B_2C$.[4] This first set of calculations yielded a reasonable model with acceptable temperature factors for all the atoms. Attempts to refine the occupancies of the atoms showed that all sites are fully occupied. Similarly, models allowing disordering of the nickel and boron atoms did not show significant mixing of these two atomic species. The final results of these refinements are given in the top of Table II, and selected interatomic distances are listed in the bottom of Table II. The plot of calculated and observed intensities is shown in Fig. 2 for the experiment at 10 K. The unit cell of the nuclear structure is represented schematically in Fig. 3(a).

B. Refinement of the magnetic structure at 5.1 and 2.2 K

The magnetic reflections appear first at a temperature of about 8 K. Generally, they form clusters of three peaks like the one illustrated in Fig. 4 which occurs at a 2θ angle of about 8°. When indexed in terms of the nuclear unit cell, the central peaks at each cluster have integral indices h,k,l which obey the condition $h+k+l=2n+1$, while reflections for which $h+k+l=2n$ are absent. These observations allow us to conclude that (i) there is no overlapping of the nuclear and magnetic reflections; (ii) the central peaks in each cluster are generated by antiferromagnetic ordering of the spins

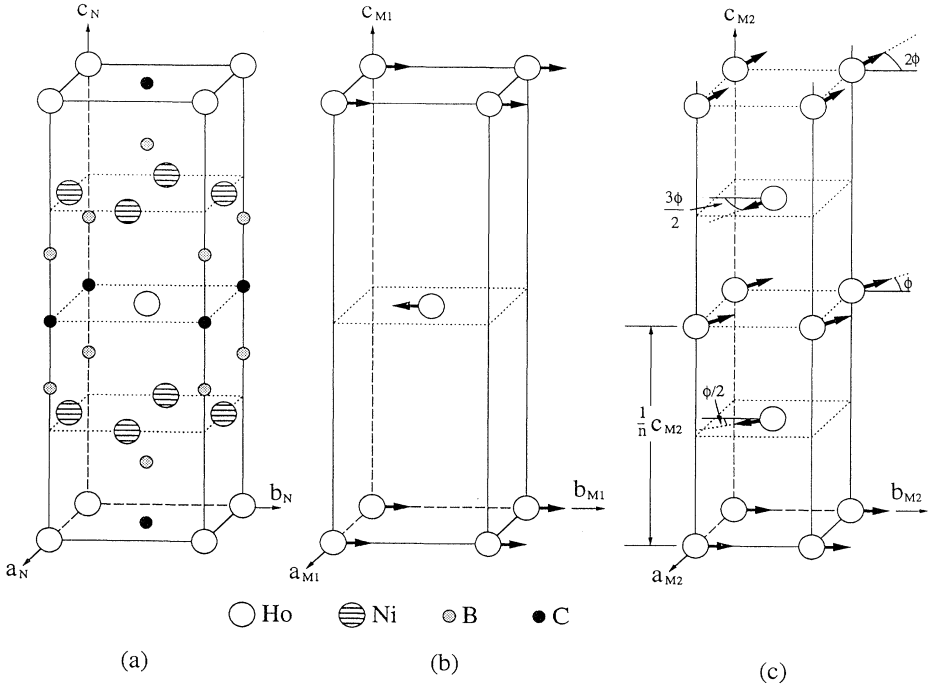

FIG. 3. Schematic representation of (a) the unit cell of the nuclear structure of $HoNi_2B_2C$; (b) the antiferromagnetic ordering of the spins of the holmium atoms; and (c) the spin configuration of the magnetic helicoidal structure. For clarity, in (b) and (c) only the holmium atoms are indicated. In (b) the moments are depicted along the *b* axis for clarity only (the *a* and *b* axes are equivalent in the tetragonal system).

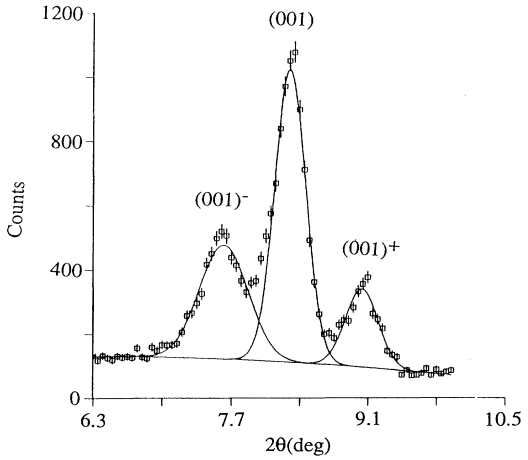

FIG. 4. Cluster of the magnetic reflection (001) with the satellites $(001)^-$ and $(001)^+$ measured at 5.1 K with $\lambda=1.539$ Å. The fitted full width at half maximum of the satellites is 0.58° and 0.40°, compared to 0.37° for the central peak.

of the holmium atoms; (iii) the antiferromagnetic coupling occurs along the c axis of the unit cell. In the tetragonal system, the magnetic reflections $00l$ have maximum intensity when the moments are perpendicular to the unique axis c, with the intensity decreasing to zero as the angle ϵ between c and the moments decreases from 90° to 0°. Inspection of the powder pattern shows that the antiferromagnetic reflection 001 at $2\theta=8.3$, for example, is very strong, thus eliminating the possibility that the moments may lie along or in the proximity of c. Intensity ratios sensitive to the spin orientation such as $I(102)/I(001)$, $I(005+104)/I(001)$, and $I(113)/I(001)$ have observed values of 0.23(2), 0.17(2), and 0.09(1), respectively. The corresponding values calculated assuming $\epsilon=90°$ are 0.22, 0.20, and 0.12, while for $\epsilon=60°$ one obtains 0.29, 0.22, and 0.16, respectively. These results, as well as the final refinement, show unambiguously that the Ho spins lie on the a-b plane, a conclusion consistent with the results of field-dependent experiments discussed in Ref. 9. We may therefore assume as a model of the antiferromagnetic structure the spin configuration schematically represented in Fig. 3(b), with the moments parallel to the a-b plane (and arbitrarily oriented along the b axis of the unit cell).

As shown in Fig. 4, there are satellite reflections on either side of the central antiferromagnetic peaks. Upon cooling, initially these three peaks have approximately the same intensity and grow at the same rate. The angular positions of the satellites are approximately temperature independent until the reentrant superconducting transition is reached. Below 5 K the commensurate central peaks grow rapidly in intensity, while the intensities of the satellites decrease sharply and shift weakly toward the central peaks, becoming barely observable at low temperatures, as shown in the top plot of Fig. 1. The presence of the satellites indicates that at all temperatures there is a modulation superposed on the commensurate ordering described previously. As mentioned above, the satellites are associated with the reflections of the antiferromagnetc structure, indicating that the modulation must affect the antiparallel ordering of the holmium spins along the c axis. This may occur either as a rotation of the spins in planes parallel to the a and b axes with formation of a helicoidal configuration, or as a variation of the magnitude of the magnetic moments, resulting in a spin-density wave. Since these two types of modulation generate the same powder reflections, neither of them can be excluded *a priori*. However, in view of the propensity of the moments to be in the a,b plane, and because of the ferromagnetic interactions within these planes, the most likely model for the modulation is a helicoidal configuration in which successive ferromagnetic planes perpendicular to c are rotated by a constant angle away from the antiparallel direction. The satellites are incommensurate with the nuclear reflections, but are approximately displaced from the positions of the antiferromagnetic reflections by a reciprocal-lattice vector $(0,0,\frac{1}{12})$ at 5.1 K, and $(0,0,\frac{1}{14})$ at 2.2 K. This means that the angle $\phi/2$ of the helicoidal rotation is about 15° and 12.9° for the two temperatures, respectively, and the wavelength of

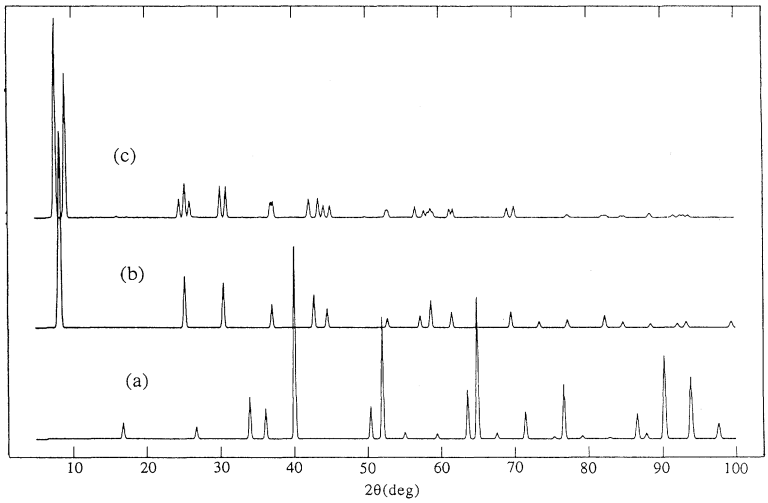

FIG. 5. Calculated profiles of the (a) nuclear; (b) commensurate antiferromagnetic; and (c) incommensurate spiral structures of $HoNi_2B_2C$ at 5.1 K.

the modulation is about 12 and 14 times the c parameter. The model of the modulated structure adopted in our refinements [Fig. 3(c)] assumes as an approximation these commensurate values.

In Fig. 5, the calculated patterns of the nuclear, antiferromagnetic and spiral structures are compared to each other. As we have noted before, and as shown in this figure, there is no overlapping of the nuclear and magnetic reflections, and, at least for the data at 5.1 K, most of the satellites can also be separated from the central reflections. This situation allows one to refine each structure separately, by excluding from the refinement the angular regions affected by the intensities of the phases not being considered. The parameters of the nuclear structure at 5.1 and 2.2 K [top of Table II, last two columns] were obtained by excluding the magnetic reflections and

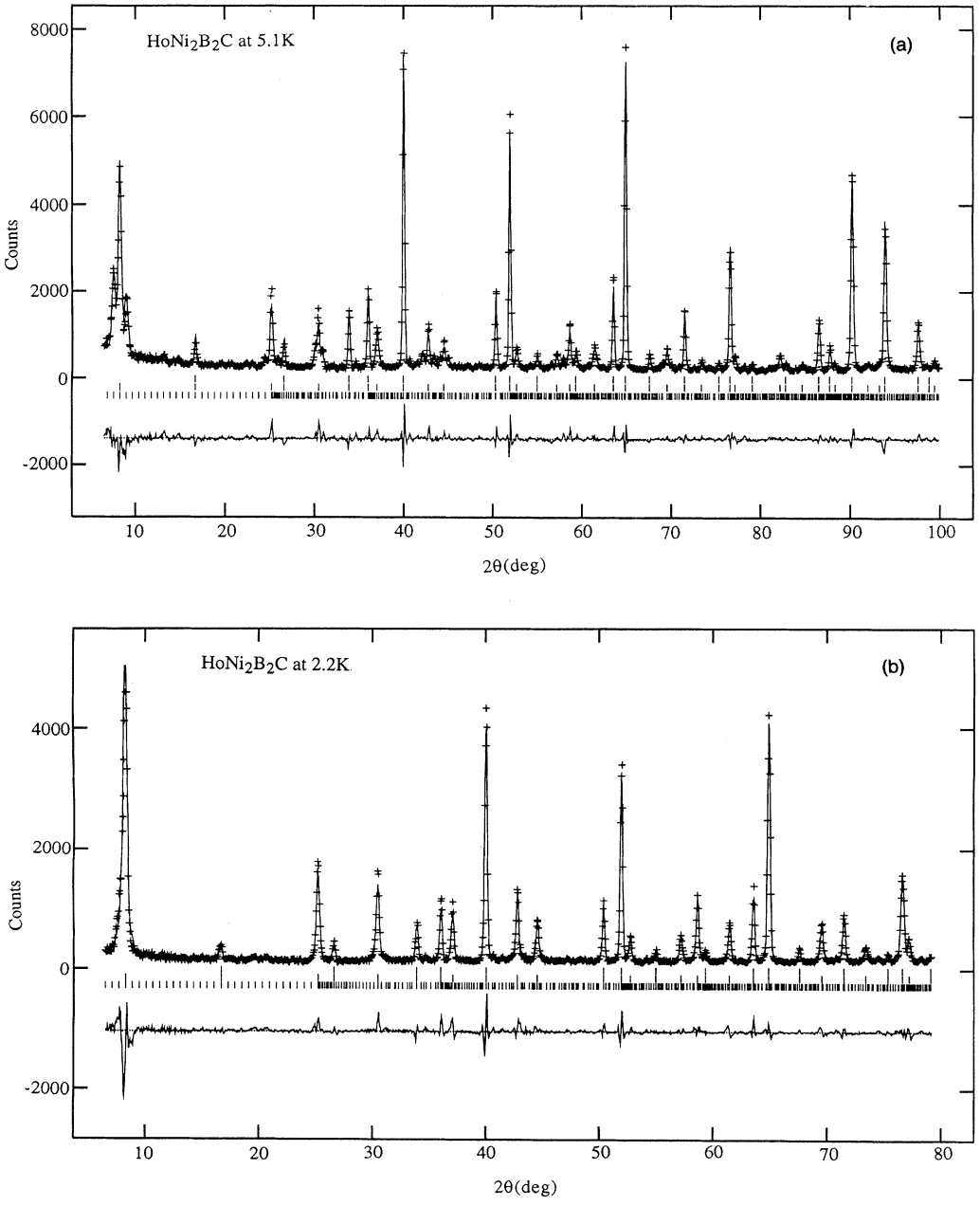

FIG. 6. Plot of observed and calculated intensities for the patterns taken at (a) 5.1 K; and (b) 2.2 K. The difference plots are shown in the lower part of the figures. The marks indicate, from top to bottom, the calculated angular positions of possible reflections of the nuclear, antiferromagnetic and spiral structures. The large number of marks in the pattern of the spiral structure is a consequence of the fact that the approximation made in this case uses a unit cell with a c parameter 12 and 14 times that of the nuclear structure.

using as initial model the one obtained at 10 K. The good agreement between observed and calculated intensities after these refinements shows that there are no detectable transitions of the nuclear structure associated with the magnetic or superconductivity ordering down to a temperature of 2.2 K.

Refinements of the models of Figs. 3(b) and 3(c) were carried out adopting the calculated magnetic form factor for holmium given in Ref. 12. The inclusion of the magnetic intensities, however, resulted in unacceptably high values of the agreement factors and in abnormal values of the lattice constants and of the instrumental zero point. The reason for such behavior was identified by noting that the full width at half maximum of the satellite reflections is significantly larger than that of either the commensurate antiferromagnetic or the nuclear peaks, and thus the same profile parameters cannot be used for the two sets of reflections. This problem is apparent in the cluster of the 001 reflections illustrated in Fig. 4, and may indicate either that spirals with slightly different values of the rotation angle ϕ coexist in the structure, or that the domains with spiral structure are sufficiently small to broaden the satellite reflections. To circumvent this problem, the antiferromagnetic and modulated structures were refined as two separate phases. In order to reduce the number of variables, the parameters of the nuclear structure were kept fixed at the values obtained previously with the magnetic reflections omitted. The high angle data were also omitted from these refinements since the intensities of the magnetic reflections become small as 2θ increases. The results of these refinements are given in the middle of Table II, and in Fig. 6 are shown the plots of observed and calculated intensities for the 5.1 and 2.2 K experiments, respectively.

As shown in the middle of Table II, the ordered moment for Ho at 2.2 K is $8.7(1)\mu_B$. This is substantially below the free-ion value of $10\mu_B$, indicating that crystal-field effects are important in this system, as confirmed by inelastic neutron scattering.[13] The intensity of the satellite peaks is only 4% of the antiferromagnetic reflections, demonstrating that the antiferromagnetic structure is dominant at low temperatures.

DISCUSSION

The nuclear structure of $HoNi_2B_2C$ [Fig. 3(a)] may be described by means of the layer sequence:

$$\cdots[(HoC)_{oc}(B)_c(Ni_2)_{xy}(B)_o(HoC)_{co}(B)_o(Ni_2)_{xy}(B)_c](HoC)_{oc}\cdots \quad (1)$$

in which the chemical composition of each layer is expressed by the symbols included in parentheses and the subscripts o and c indicate if the atoms are located at the origin or at the center of the mesh, respectively. The subscripts x and y specify that one of the Ni atoms of the (Ni_2) layers is located at $\frac{1}{2}$ along the a axis and the other at $\frac{1}{2}$ along the b axis. The layers contained in one unit cell are enclosed in square brackets.[14] Sequence (1) may be regarded as formed by (HoC) layers with the configuration of the rocksalt structure, alternating with $(B)(Ni_2)(B)$ blocks, having a fluorite-type arrangement of the atoms with the Ni layer sandwiched between the two boron planes.

As apparent from Fig. 3(a), boron is coordinated by four Ni atoms, at a distance of 2.099 Å, forming the base of a pyramid having at its apex a carbon atom with a B-C separation of 1.485 Å. Holmium is 12 coordinated, with eight B atoms at 2.896 Å forming a prismatic cage, and with four carbon atoms located on the same layer at a Ho-C distance of 2.486 Å. Carbon is at the center of a distorted octahedron, surrounded by four Ho atoms on the same plane and by two apical B atoms. Finally, Ni is coordinated by four B atoms having a tetrahedral configuration and by four other Ni atoms on the same plane with a Ni-Ni separation of 2.486 Å. The layers are connected to each other along c by the B-C and B-Ni bonds, while the connections with the layers are provided by the Ho-C and Ni-Ni bonds.

By increasing in sequence (1) the number of the rocksalt layers from one to two, we obtain the sequence:

$$\cdots[(HoC)_{oc}(B)_c(Ni_2)_{xy}(B)_o(HoC)_{co}](HoC)_{oc}\cdots \quad (2)$$

corresponding to a compound of formula HoNiBC. The Lu analog of this material has in fact been prepared and characterized by Siegrist *et al.*[4] By extending this process to n layers, we form a homologous series of general formula $Ho_nNi_2B_2C_n$, of which $HoNi_2B_2C$ and HoNiBC are the first and second members, respectively. In their paper, Siegrist *et al.* discuss the possibility of forming a second homologous series by adding NiB layers with Ni and B in the ratio 1:1. This interesting suggestion would result in compounds with general formula $HoNi_{2n}B_{2n}C$ having adjacent boron layers connected either as indicated in the sequence:

$$\cdots(B)_c(Ni_2)_{xy}(B)_o(B)_c(Ni_2)_{xy}(B)_o\cdots \quad (3)$$

or in the sequence

$$\cdots(B)_c(Ni_2)_{xy}(B)_o(B)_o(Ni_2)_{xy}(B)_c\cdots . \quad (4)$$

In the first case, the separation of the boron atoms would be greater than 2.5 Å, i.e., too large to form a strong B-B bond and a stable structure. In the second case, the boron atoms would be located on top of each other along the c axis. If we assume a B-B separation of about 1.8 Å, as found in boranes, the structure could be held together by these bonds, and the distance between two consecutive (Ni_2) layers would approximately be 4 Å. Thus far, no members beyond $LuNi_2B_2C$ and LuNiBC have been prepared, but it would be interesting to investigate the structural and electronic properties of compounds with

short distances between (Ni_2) layers. It is worth recalling at this point that the thallium and bismuth superconductors also form homologous series having rocksalt and perovskite blocks of variable thickness interleaved along the long axis of the unit cell.[15] The magnetic properties of $HoNi_2B_2C$ and, in particular, the relationship between magnetic structure and observed magnetic and superconducting transitions, has been analyzed in detail in Ref. 9 and will not be discussed any further here.

ACKNOWLEDGMENT

Work in the Center for Superconductivity at the University of Maryland was supported in part by the NSF, DMR 93-02380.

[1]R. Nagarajan, C. Mazumdar, Z. Hossain, S. K. Dhar, K. V. Gopalakrishnan, L. C. Gupta, C. Bodart, B. D. Padalia, and R. Vijayaraghavan, Phys. Rev. Lett. **72**, 274 (1994).

[2]R. J. Cava, H. Takagi, H. W. Zandbergen, J. J. Krajewski, W. F. Peck, Jr., T. Siegrist, B. Batlogg, R. B. van Dover, R. J. Felder, K. Mizuhashi, J. O. Lee, E. Eisaki, and S. Uchida, Nature **367**, 252 (1994).

[3]R. J. Cava, H. Takagi, B. Batlogg, H. W. Zandbergen, J. J. Krajewski, W. F. Peck, Jr., R. B. van Dover, R. J. Felder, T. Siegrist, K. Mizuhashi, J. P. Lee, H. Eisaki, S. A. Carter, and S. Uchida, Nature **367**, 146 (1994).

[4]T. Siegrist, H. W. Zandbergen, R. J. Cava, J. J. Krajewski, and W. F. Peck, Jr., Nature **367**, 254 (1994).

[5]W. A. Fertig, D. C. Johnston, L. E. Delong, R. W. McCallum, M. B. Maple, and B. T. Mattias, Phys. Rev. Lett. **38**, 987 (1977).

[6]M. Ishikawa and O. Fischer, Solid State Commun. **23**, 37 (1977).

[7]H. Eisaki, H. Takagi, R. J. Cava, K. Mizuhashi, J. O. Lee, B. Batlogg, J. J. Krajewski, W. F. Peck, Jr., and S. Uchida, Phys. Rev. B **50**, 647 (1994).

[8]J. A. Gotaas, J. W. Lynn, R. N. Shelton, P. Klavins, and H. F. Brown, Phys. Rev. B **36**, 7277 (1987).

[9]T. E. Grigereit, J. W. Lynn, Q. Huang, A. Santoro, R. J. Cava, J. J. Krajewski, and W. F. Peck, Jr., Phys. Rev. Lett. **73**, 2756 (1994).

[10]L. Koester, H. Rauch, E. Seymann, and H. Bittermann, *Table of Neutron Scattering Lengths* (Neutron News and Breach Science Publishers, New York, 1992).

[11]A. C. Larson and R. B. Von Dreele, General Structure Analysis System, Report LA-UR-86-748, Los Alamos National Laboratory, Los Alamos, NM 87545 (1990).

[12]M. Blume, A. J. Freeman, and R. E. Watson, J. Chem. Phys. **37**, 1245 (1962).

[13]T. E. Grigereit and J. W. Lynn (unpublished).

[14]A. Santoro, J. Alloys Compounds **197**, 153 (1993).

[15]S. A. Sunshine and T. A. Vanderah, in *Chemistry of Superconductor Materials,* edited by T. A. Vanderah (Noyes, Park Ridge, NJ, 1992), p. 257.